Research Article

Synthetic Type III-E CRISPR-Cas Effectors for Programmable RNA-targeting

Daniel J. Brogan [1,†], Calvin P. Lin [2,†], Elena Dalla Benetta [1], Tianqi Wang [1], Fangying Chen [1], Harry Li [2], Claire Lin [1], Elizabeth A. Komives [2,*], and Omar S. Akbari [1,*]

*1 - **School of Biological Sciences,** Department of Cell and Developmental Biology, University of California San Diego, La Jolla, CA 92093, USA*

*2 - **Department of Chemistry and Biochemistry,** University of California San Diego, La Jolla, CA 92093-0309, USA*

***Correspondence to Elizabeth A. Komives and Omar S. Akbari:** ekomives@ucsd.edu (E.A. Komives), oakbari@ucsd.edu (O.S. Akbari)*
https://doi.org/10.1016/j.jmb.2025.169566
Edited by M.F. Summers

Abstract

The recent discovery of the type III-E class of CRISPR-Cas effectors has reshaped our fundamental understanding of CRISPR-Cas evolution and classification. Type III-E effectors are composed of several Cas7-like domains and a single Cas11-like domain naturally fused together to create a single polypeptide capable of targeting and degrading RNA. Here we identified a novel type III-E-like effector composed of three Cas7 domains and a Cas1 domain which was not active but could be engineered into an active chimeric RNA-targeting Cas effector by domain additions and swaps from other type III-E effectors. The results reveal that various domains in type III-E effectors can be swapped for the equivalent domain from a different type III-E effector. Remarkably, the Cas1 domain located at the C-terminus of Cas7-1 could be swapped in place of the Cas11 domain located between the Cas7.1 and the Cas7.2 domains of *Di*Cas7-11. The results reveal a new modality for engineering type III-E effectors from the blueprints found in nature.

Introduction

The continuous evolution of CRISPR-Cas systems has resulted in the discovery and engineering of revolutionary genome engineering technologies. Recently, the type III-E CRISPR-Cas system was discovered [1] and characterized [2,3]. Type III-E effectors are nominally class 1 CRISPR-Cas systems, which typically utilize a multiprotein complex to accomplish DNA- and/or RNA-targeting [1], but are similar to class 2 CRISPR-Cas systems as they utilize a single protein that accomplish the same functions. Type III-E Cas effectors accomplish programmable RNA-targeting by employing a single, large protein composed of four Cas7-like domains, one Cas11 domain, and a large insertion (INS) domain, hence being named Cas7-11 [4,5] (or gRAMP for giant Repeat Associated Mysterious Protein [6]). Recent studies have demonstrated that type III-E effectors are capable of programmable RNA knockdown in prokaryotic and eukaryotic cells and do not exhibit RNA collateral cleavage activity that typically limits applications of CRISPR-Cas13 systems [7–10]. Cas7-11 target binding activates a downstream caspase activity that results in cell dormancy, or death, and appears to serve as the primary immune response for type III-E CRISPR-Cas systems [6,11,12]. When expressed in the absence of their caspase signaling pathway, type III-E effectors are highly specific ribonucleases. Recently, a smaller Cas7-11 (Cas7-11S) protein was engineered through deletion of the INS domain and replacement with a GS-linker [5]. With the goal of exploring which domains are required for activity in other type III-E CRISPR-Cas effectors, we pursued a combination of bioinformatics and orthologous domain swapping studies.

Cas7-11 is composed of Cas7 domains, (Cas7.1-7.4), a Cas11 domain, the insertion domain (INS), and a Carboxy-terminal extension domain (CTE) that are fused together through 4 linkers [5]. The Cas7.1 domain processes the pre-crRNA by cleaving it at position -15 and recognizes and linearizes the 5′-tag of the direct repeat (DR), while the Cas7.2-7.4 domains and the INS recognize the spacer region of the crRNA and the complementary tgRNA [4,6,13]. The Cas11 domain has been shown to be necessary for positioning the tgRNA for cleavage [5,6,13]. The Cas7.2 and Cas7.3 domains have a conserved Asp residue responsible for tgRNA cleavage [5]. The Cas7.4 domain is also required for activity but may play a more structural role [5,13].

The hypothesis that type III-E effectors may constitute natural fusions of modular proteins with interchangeable orthologous domains is attractive for engineering new RNA cleavage activities within this family of proteins. Through bioinformatics analysis, we identified a small member of the family and named it Cas7-1, but this protein did not demonstrate RNA cleavage activity. To explore the relationship between size, structure, and function of modular Cas proteins, chimeras were generated varying the origin and location of Cas domains within the modular framework. By generating a panel of 52 variants, the modularity of the functional domains in these proteins was further defined. The missing functions in the Cas7-1 were modularly reintroduced resulting in novel active type III-E effectors.

Results

Sequence alignments reveal catalytic and structural features of the Cas7-1 protein

An initial bioinformatic search and alignment was performed to identify single polypeptide effectors with novel Cas7-based architectures to identify variants with possible novel architectures. An initial BLAST search using the *Desulfonema ishimotonii* Cas7-11 (*Di*Cas7-11) sequence revealed a hit for an unusual type III-E protein denoted as a Cas1 nuclease (MBU1487208.1). Analysis of the domain architecture of this protein using HHPred revealed a single polypeptide chain with linked domains that aligned well to Cas7 and Cas1 domains, showing the protein to be composed of three Cas7-like domains and one Cas1 nuclease domain (Table S1). The new protein was named Cas7-1. The genomic sequence of Cas7-1 was identified in a ground water sample from Sweden (BioSample: SAMN19298298; Sample name: Old_saline.mb.48) and it remains unknown what bacterial strains harbor this sequence or what its function is. With the goal of finding smaller domains, analysis of the domain sizes of known type III-E effectors with activity verified in mammalian cells (Table S2) showed that, along with Cas7-1, *Di*Cas7-11 and *Hydrothermal vent sediment* Cas7-11 (*Hvs*Cas7-11) domains were the smallest across the set of orthologs. The amino acid sequences are provided in Table S3.

Cas7-1 was then assessed for activity against target ssRNA. A search for possible crRNAs associated with Cas7-1 revealed a 38 nt consensus direct repeat (DR). Secondary structure predictions of the forward and reverse directions of the consensus DR (Figure S1A, B) showed that the reverse direction contains a similar stem-loop structure to the DR of *Di*Cas7-11 (Figure S1B, C). However, tests of Cas7-1 targeted cleavage activity with both the 5′ and 3′ orientations of the two DR sequences exhibited no target ssRNA cleavage (Figure S1D).

Sequence alignments of Cas7-1 showed that it lacked an INS domain which is found in all known type III-E effectors (Figure 1A) [3]. The Cas7-1 Cas7.3 domain retained a conserved catalytic residue found in all known Cas7.3 domains (Figure 1B), as well as zinc-finger motifs unique to type III-E effectors (Figure 1C) [5]. However, the alignments revealed that Cas7-1 is missing a portion of the N-terminus, including a CRISPR RNA (crRNA) processing domain (Cas7.1) and the N-terminal half of the Cas7.2 domain including the catalytic residue, which likely explains the lack of activity. The Cas7-1 Cas1 domain aligned to an accessory Reverse Transcriptase-Cas1 (RT-Cas1) fusion protein commonly associated with type III systems of all characterized subtypes (III-A, III-B, III-C, and III-D, but not III-E) [14,15] (Figure 1D). In these systems, the active Cas1 domain is required for adaptation of new spacers from interfering RNA [16]. Given its ability to interact with RNA, we hypothesized that this Cas1 domain could also facilitate crRNA/tgRNA interaction [17].

Orthologous domain substitution to resurrect activity of Cas7-1

In an attempt to rescue activity of the Cas7-1 protein, domains from the active *D. ishimotonii*, Cas7-11 (*Di*Cas7-11) were incorporated and/or substituted based on aligned domains from type III-E effectors, a process that we call Orthologous Domain Substitution (ODS) [18]. Predicted structures of the Cas7-1 domains from AlphaFold2 [19–21] were aligned to the solved structure of *Di*-Cas7-11 to aid in downstream engineering

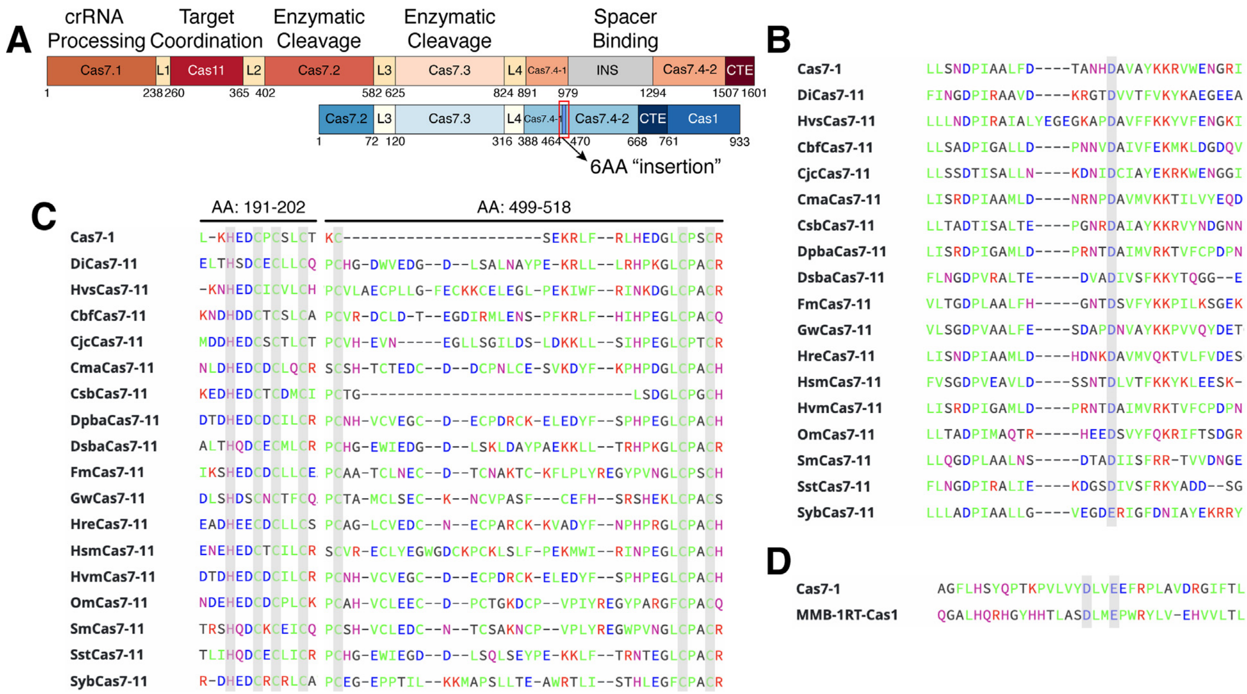

Figure 1. Cas7-1 sequence and predictive structure in relation to type III-E effectors. (**A**) Schematic representation of a typical Cas7-11 architecture (red) and the architecture of Cas7-1 (blue). (**B**) Alignment of catalytic residue in the Cas7.3 domain of Cas7-1 against published Cas7-11 proteins (*3*). (**C**) Alignment of zinc finger residues in the Cas7.2 and Cas7.3 domains of Cas7-1 and Cas7-11 proteins. Amino Acid (AA) position represents position in Cas7-1 protein sequence. (**D**) Alignment of Cas1 domain of Cas7-1 to MMB1 RT-Cas1 fusion protein (NCBI Ascension here). Highlighted sections represent catalytic residues of Cas1, where E847 of Cas7-1 aligns to E870 of MMB1 RT-Cas1.

[5,13,22,23]. An initial set of 16 different effectors (hereafter referred to as sCas7 variants) with different domain and linker substitutions were generated while also varying the overall architecture based on Cas7-1 or Cas7-11 proteins (Figure 2A). Since Cas7-1 was missing a Cas7.1 domain known to be required for binding to the DR [4], the Cas7.1 domain from *Di*Cas7-11 was added onto the N-terminus of the Cas7-1 variant. Cas7-1 is also missing the first half of the Cas7.2 domain so in the first three variants, the first half of the *Di*Cas7-11 Cas7.2 domain was fused to the partial C-terminal Cas7.2 domain of Cas7-1 using varied linkers. The activity of the sCas7 variants was assayed by measuring knockdown of EGFP mRNA in HEK293T cells. The cells were transfected with three plasmids; one encoding EGFP, a second encoding a crRNA that contains a DR recognized by *Di*Cas7-11 with spacer sequences targeting EGFP for down-regulation (Table S4), and a third plasmid encoding one of the variant sCas7 effectors. RNA-knockdown activity was observed by a reduction in fluorescent signal relative to a non-targeting crRNA control and confirmed through RT-qPCR (Figure 2B). This assay showed that sCas7v1-v3 had some RNA knockdown ability, suggesting that appending a Cas7.1 and partial Cas7.2 domain to Cas7-1 was sufficient for rescuing the activity of Cas7-1. Next, the Cas7-1 partial Cas7.2 domain was replaced with the entire Cas7.2 domain of *Di*Cas7-11 to generate sCas7v4 and v5 which differed only by inclusion of L2 for sCas7v5 (Figure 2). While sCas7v4 was not active, sCas7v5 showed knockdown activity similar to sCas7v1-3. It is possible that the presence of both L1 and L2 in sCas7v5 helped position the domains for activity, but this remains speculation. Next, the Cas7.3 and/or Cas7.4 domains including the INS domain of *Di*Cas7-11 were substituted for the same respective domains in Cas7-1 to generate sCas7v6 and v7. These variants showed similar activity as variants 1–3 and 5.

RT-qPCR confirmed that variants with the Cas1 domain from Cas7-1 at the C-terminus were active in RNA knockdown despite the fact that they lacked the Cas11 domain which is understood to be required for target RNA cleavage in type III-E effectors [5,6]. In addition, the Cas1 domain at the C-terminus supports RNA cleavage activity in lieu of a Cas11 domain regardless of whether the Cas7 domains are from *Di*Cas7-11 or Cas7-1 (Figure 2). This came as a surprise as the Cas1 and Cas11 domains are not related either in sequence, structure, or function (Table S3) [5,16].

*Di*Cas7-11 has the INS domain inserted within the Cas7.4 domain whereas Cas7-1 has a six amino acid insertion in a similar place. The sCas7v7

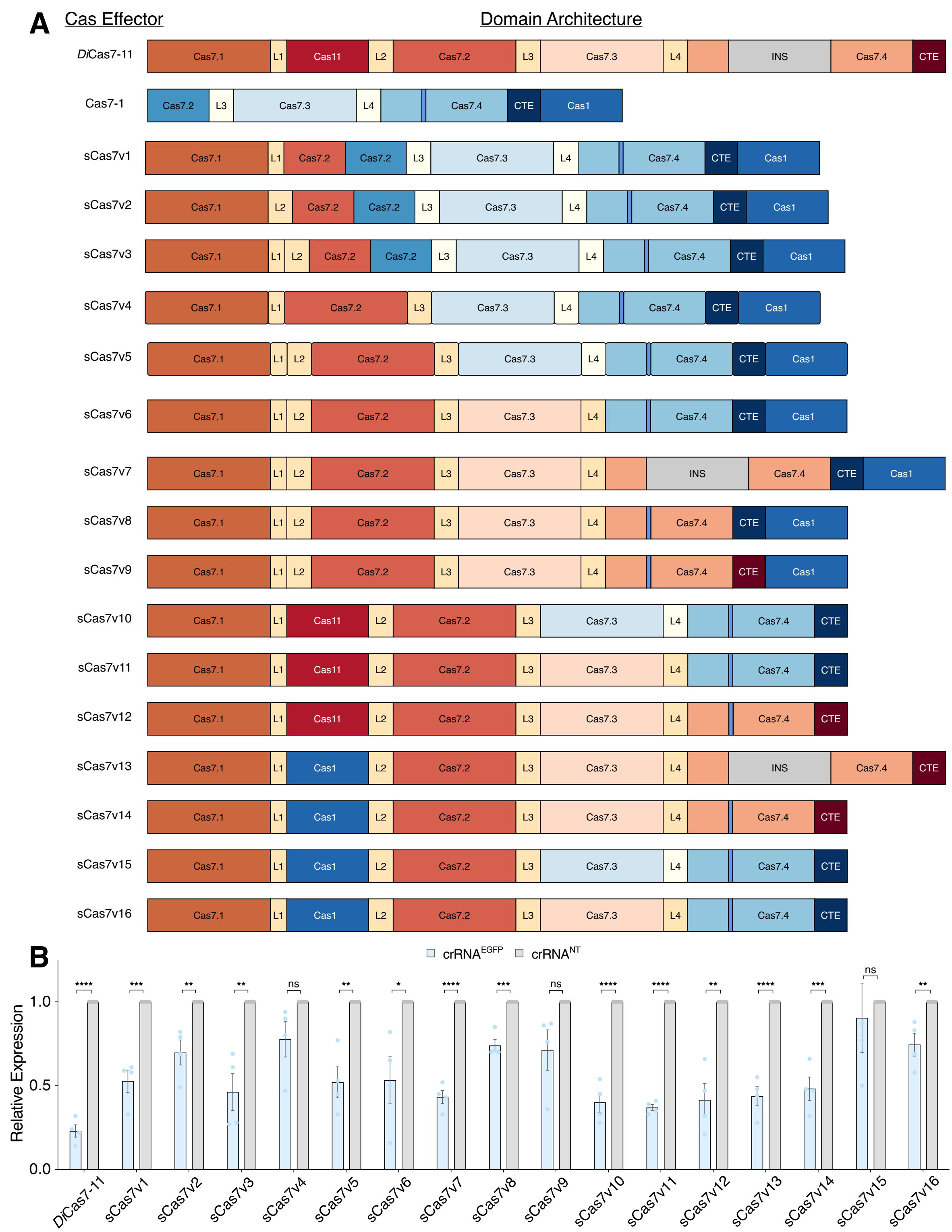

Figure 2. Construction and analysis of initial Cas7 variants. (**A**) Schematic representing the construction method for initial sCas7 variants. Red lines represent domains from DiCas7-11 and blue lines represent domains from Cas7-1. The chimeric Cas7 proteins are called sCas7. (**B**) qPCR analysis of EGFP targeted knockdown with sCas7 variants that have a C-terminal orientation of the Cas1 domain and sCas7 variants that orient the Cas11 or Cas1 domain internally as in the Cas7-11 architecture.

contained the *Di*Cas7-11 INS domain which was replaced with the 6 amino acid insertion sequence from Cas7-1 to generate sCas7v8. To generate sCas7v9, the *Di*Cas7-11 CTE was replaced with the Cas7-1 CTE. Although sCas7v7 had activity, sCas7v8 and v9 had poor RNA knockdown activity, suggesting that the INS domain was contributing to activity in this context. Thus, most of the variants (Cas7v1-3,5-8) with a Cas1 domain positioned at the C-terminus and no Cas11 domain retained RNA knockdown activity. These results led to the surprising conclusion that Cas1 can serve as a substitute for the Cas11 domain's role in properly orienting the target RNA [5,6,13,23,24].

The next set of variants were designed to reflect the architecture of *Di*Cas7-11 with the Cas11 domain between the Cas7.1 and Cas7.2 domains as it is in *Di*Cas7-11 (sCas7v10-v12). sCas7v10 had the Cas7-1 Cas7.3 domain, Cas7.4 domain, and CTE, and therefore was the most Cas7-1-like. sCas7v11 had a *Di*Cas7-11 Cas7.3 domain in place of the Cas7-1 Cas7.3 domain. sCas7v12 had both the DiCas7-11 Cas7.3 and Cas7.4 domains. All of these variants did not have the INS but instead had the 6-AA insertion sequence from Cas7-1. sCas7v10-12 all showed robust RNA knockdown activity, suggesting that substituting the Cas7.3, Cas7.4, and CTE domains from one protein to another still allowed for active type III-E effectors.

In vitro activity of DiCas7-11/Cas7-1 chimeras

We sought to further characterize variants with Cas7-1 domains and higher activity from the RNA knockdown in cells and chose sCas7v10 (Cas7.3 domain is from Cas7-1) and sCas7v12 (catalytic domains are both from *Di*Cas7-11). Notably both of these proteins generated the same sized cleavage products indicating that the Cas7.2 and Cas7.3 domains cleave in the same place regardless of their species of origin. We also attempted to study variants such as sCas7v14A but were unable to express and purify them in bacteria. We performed *in vitro* ssRNA cleavage assays with crRNAs with canonical *Di*Cas7-11 DRs (Table S4). Cleavage was observed for crRNAs with spacers between 20 and 30 nt in length. A substantial increase in both crRNA processing and target cleavage was observed as the spacers were shortened, with the best cleavage activity observed for 22–24 nt spacers (Figure S2A). The increase in cleavage activity due to spacer truncation was further substantiated by demonstrating sCas7v10-mediated knockdown of crRNA in cell culture via RT-qPCR analysis (Figure 3A). Tiling the crRNAs across the ssRNA target and incubating for 6 h to clearly visualize the complete cleavage product, we observed stepwise cleavage products demonstrating activity of both the Cas7.3 and Cas7.4 domains (Figure 3B, C). Cleavage activity was completely abolished through mutagenesis of both active sites for *Di*Cas7-11, sCas7v10, and sCas7v12 (the double mutation D429A/D654A is denoted by d), while crRNA processing activity was retained (Figure 3D, brown arrows).

The crRNA processing activity against a full array structure, containing a DR on either end of a 22-nt spacer, with the same spacer as crRNA-5 was also investigated (Figure 3E, Table S4). Neither wild-type (WT) *Di*Cas7-11 nor sCas7v12 could completely process an array structure into a mature 37 nt crRNA, but instead yielded an incompletely processed 57 nt product with a 15 nt DR 5′ to the spacer and a 20 nt remnant 3′ to the spacer (Figure 3F). As we reported recently, this lack of complete processing was not known because most previous *in vitro* studies used a pre-crRNA with no 3′ DR and consequently no 3′ hairpin upon processing ($crRNA_{37}$) [25]. The observation that *Di*Cas7-11 is unable to process pre-crRNA aligns with observations that the ortholog *Sb*Cas7-11 is also unable to process pre-crRNA [2,23,24,26] and that the type III-A/B complexes require other nucleases for crRNA processing [27,28] (Figure 3F). The Cas7.1 domain only produces a mature 37 nt product when there is only a 5′ DR, leaving a 15-nt DR upon processing (Figure 3E). This suggests that type III-E effectors do not cleave off the 20-nt DR fragment downstream of the spacer when processing arrays (Figure 3E). However, by modifying the array structure to incorporate mature 15 nt DRs on both ends of the spacer sequence, a crRNA without excess nucleotides on the 3′ end could be obtained (Figure 3G). This experiment suggests that the 15 nt mature DR sequence rather than the 35 nt DR sequence in pre-crRNA is sufficient for recognition and processing. The full array was shown to inhibit tgRNA cleavage at the Cas7.3 domain in both WT and sCas7v12 as previously observed [25]. Moreover, it appears that because sCas7v10 contains Cas7.3/Cas7.4/CTE domains from Cas7-1, RNA cleavage activity is inhibited at both Cas7.2 and Cas7.3 active sites when the 3′ 20-nt DR fragment is present (Figure 3H). Together, these results suggest that sCas7 variants can accomplish RNA cleavage like other Cas7-11 proteins and type III-E CRISPR-Cas systems, using catalytic domains from both Cas7-1 and *Di*Cas7-11.

Variants with the Cas1 domain in between the Cas7.1 and Cas7.2 domains

The Cas11 domain from *Di*Cas7-11 was replaced with the Cas1 domain from Cas7-1 to generate sCas7v13 and replacing the *Di*Cas7-11 INS domain with the six amino acid insertion from Cas7-1 generated sCas7v14. Both of these variants also elicited RNA knockdown. Swapping the *Di*Cas7-11 Cas7.3 and/or Cas7.4 domains in sCas7v13-14 with their respective Cas7-1

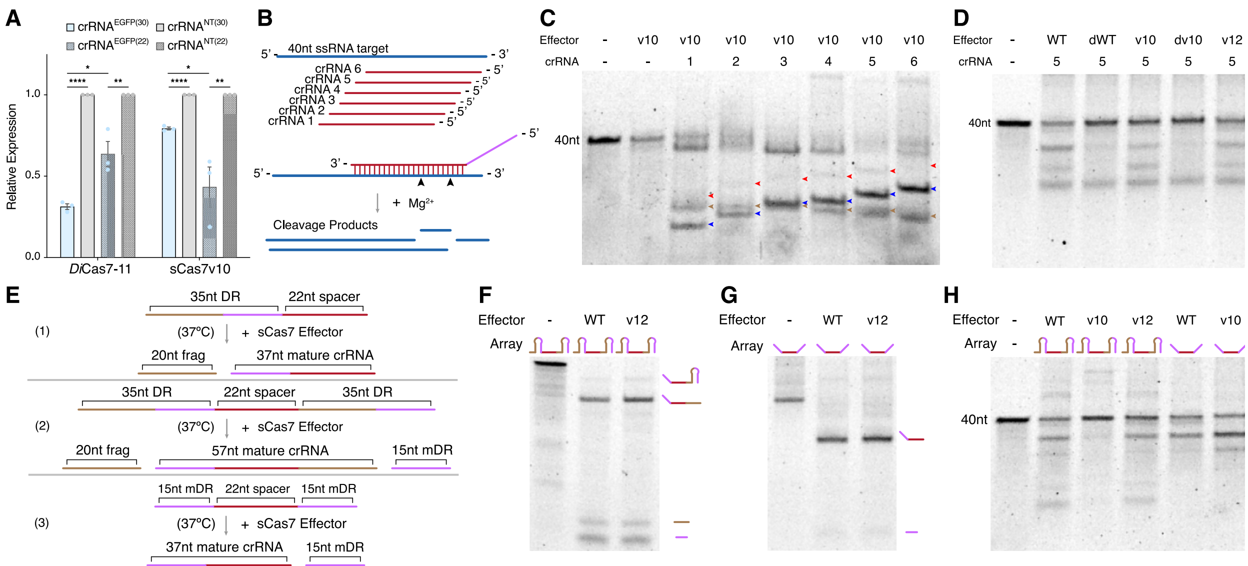

Figure 3. Cleavage activity of the sCas7 variants. (**A**) qPCR analysis of EGFP knockdown comparing 30 nt vs 22 nt spacers for DiCas7-11 and sCas7v10. Significance is calculated and determined using unpaired *t*-test between crRNA^{EGFP} and crRNA^{NT}. Error bars represent sem ($n = 3$). (**B**) Schematic depicting the crRNAs used for assessment of *in vitro* cleavage activity and depiction of cleavage and expected cleavage products. Black arrowheads represent cut sites of crRNA-5. (**C**) Experiment tiling six 22 nt crRNAs across the 40 nt ssRNA target to obtain stepwise cleavage products. (**D**) Assessment of cleavage pattern and catalytic inactivation of DiCas7-11, sCas7v10, and sCas7v12 through site specific mutagenesis (D429A/D654A indicated by d). (**E**) Schematic representation of different crRNA processing outcomes. (1) "single-guide" crRNA processing. (2) native array crRNA processing. (3) modified array crRNA processing. (**F, G**) crRNA array processing activity by DiCas7-11 (WT) and ΔINS mutant, sCas7v12. Array structures represented by schematics above each lane. crRNA processing products and approximate location on gel depicted by schematics on the side of gel. (H) Comparison cleavage assay between WT DiCas7-11, sCas7v10, and sCas7v12 (ΔINS) with varying array structures. Red arrows represent cleavage by Cas7.2 only. Blue arrows represent cleavage products by Cas7.3 or from both Cas7.2/Cas7.3 active sites cleaving the target. Brown arrows represent 20 nt processed DR fragments. Purple represents 15 nt mature DR (3′ only).

domains either abolished activity (sCas7v15) or greatly reduced it (sCas7v16). To determine why the Cas7-1 Cas1 domain in place of the *Di*Cas7-11 Cas11 domain didn't work with its own Cas7.3 and Cas7.4 domains, we aligned the Cas1 domain sequence with other Cas1 domains (Figure S3). This analysis revealed that the first 29 residues aligned to the N-terminal sequence of the RT portion of RT-Cas1 fusion proteins with an AlphaFold2 predicted disordered region followed by an α-helix (Figure 4B). Using this predicted structure, we generated two versions of the Cas1 domain with either truncation of only the disordered region (B variants) or the whole 29-residue sequence (A variants) and compared them to sCas7v14-16 (Figure 4A–C). In most cases, the constructs in which all 29 amino acids were deleted had slightly better activity (Figure 4C). These results suggested that the extra 29 residues may alter the position of the Cas1 domain with respect to the other Cas7 domains which might affect its ability to position the tgRNA.

Predicted structures suggest Cas1 is situated where Cas11 is in DiCas7-11

The observation that several sCas7 variants that lacked Cas11 and had a Cas1 domain instead retained activity was very interesting. To understand how the C-terminal Cas1 domain could substitute for the Cas11 domain which was inserted between the Cas7.1 and Cas7.2 domains, we used AlphaFold3 to generate a model of sCasv12 which corresponds to the wild type *Di*Cas7-11 without its INS (Figure 5A–C) which perfectly overlayed with the full wild-type *Di*Cas7-11 structure (PDB:7WAH) [5,6,23,24]. This "wild type" protein was compared to AlphaFold3 models of sCas7v5 (which has the Cas1 domain at the C-terminus of the protein) (Figure 5D–F) and sCas7v14a (which has the Cas1 domain in place of the Cas11 domain inserted between Cas7.2 and Cas7.3 (Figure 5G–I). Comparing Figure 5B, E, and H shows that AlphaFold3 predicts these proteins with similar pLDDT scores despite the fact that two of them contain a Cas1 domain

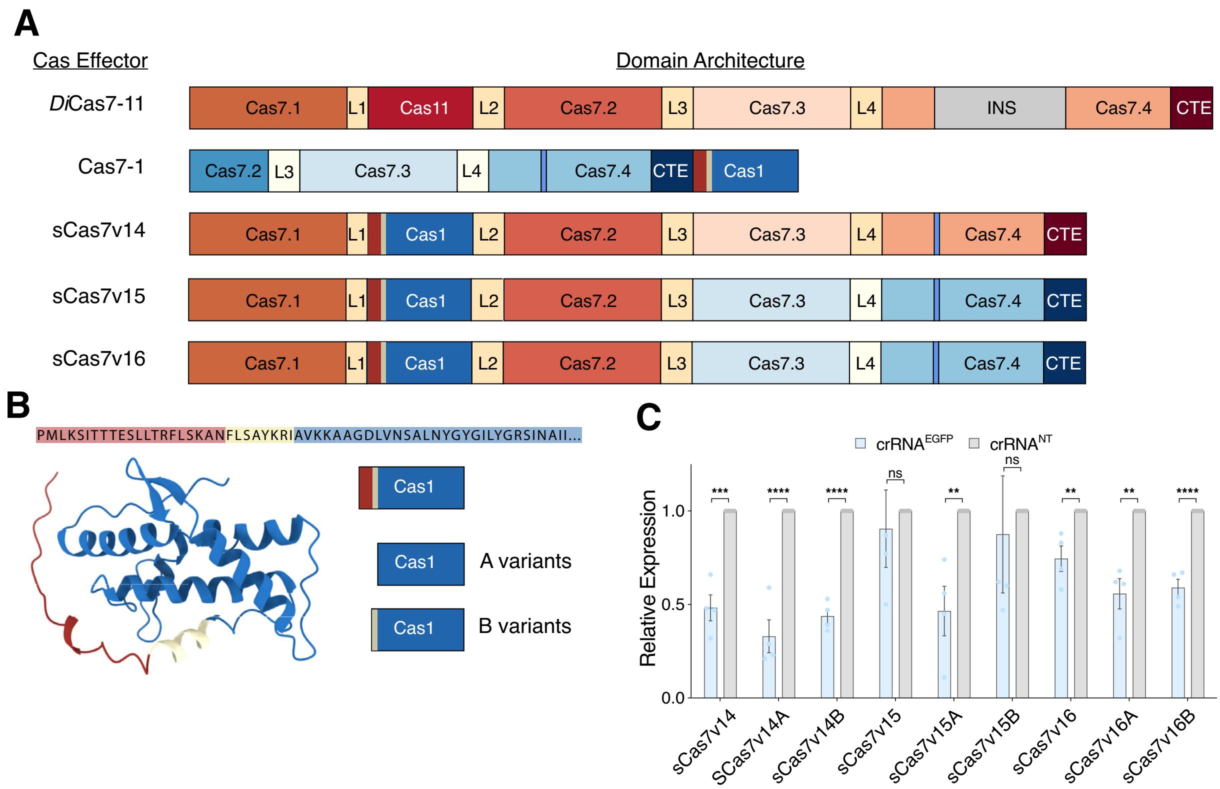

Figure 4. N-terminal truncations of the Cas1 domain. (**A**) Schematic showing the domain organization of the N-terminal truncated variants. Regions in red and tan indicate sequences from Cas1 that were deleted. (**B**) Alpha Fold 2 model of the Cas1 domain showing the N-terminal disordered segment (red, 21 AA and tan, 8 AA) corresponding to the two modes of truncation. (**C**) qPCR analysis quantifying EGFP knockdown by sCas7 variants with different truncations of Cas1. In all qPCR plots, significance is calculated and determined using unpaired *t*-test between crRNA^{EGFP} and crRNA^{NT}. Error bars represent sem (n = 4).

(which is not similar either in sequence or in structure to the Cas 11 domain) instead of a Cas11 domain and the Cas1 domain is in two different locations in the primary sequence. In the wild-type structure, the Cas11 domain abuts the Cas7.2 and Cas7.3 active site and provides key residues that likely assist in catalysis of RNA cleavage at the flipped bases in the tgRNA (Figure 5C, F, I) [5]. Remarkably, in the sCas7v5 model, the CTE domain allows the C-terminal Cas1 domain to be positioned similarly to the Cas11 domain in the wild-type protein (Figure 5E). In the sCas7v14a, which has the Cas1 domain in place of the DiCas7 Cas7.2 and Cas7.3 domains, the Cas1 domain is predicted to be positioned where the Cas11 domain is in the wild type protein. In both the sCas7v5 and sCas7v14a models, basic residues within the Cas1 domain are near the flipped bases hinting at why this domain substitution may result in an active protein (Figure 5C, F, I).

Combining domains from DiCas7-11, HvsCas7-11, and Cas7-1 to reduce size while maintaining RNA targeting

A set of 36 additional sCas7 variants were generated using the ODS method to systematically combine domains from three effectors (*Di*Cas7-11, *Hvs*Cas7-11, and Cas7-1) (Figure S4). To streamline the design method and reduce the overall size of the effectors, we included the Cas7.4 domain from Cas7-1 in all the additional sCas7 variants and used *Di*Cas7-11 linkers, except when *Hvs*Cas7.1 and *Hvs*Cas11 were used together. The additional effectors varied in size from 1233 to 1292 amino acids in length, marginally decreasing the size of type III-E effectors relative to ΔINS *Di*Cas7-11 (1286 AA) [5].

The RNA knockdown capabilities of the additional sCas7 variants were assessed using the previously described reporter assay in HEK293T cells, and RNA knockdown was quantified using RT-qPCR. We found that sCas7 variants containing the *Di*Cas7.1 domain resulted in consistent EGFP knockdown comparable to *Di*Cas7-11, whereas effectors containing the *Hvs*Cas7.1 domain demonstrated little-to-no knockdown activity (Figure 6A) despite using an *Hvs* crRNA. When *Di*Cas7.1 was included in the protein and the *Di*Cas7-11 crRNA was used, variants with a *Di*Cas11- or *Hvs*Cas11 domain slightly outperformed variants with a Cas1 domain in place of the Cas11 domain (Figure S5D). Variants sCas7v35, sCas7v39 (both with the *Di*Cas11

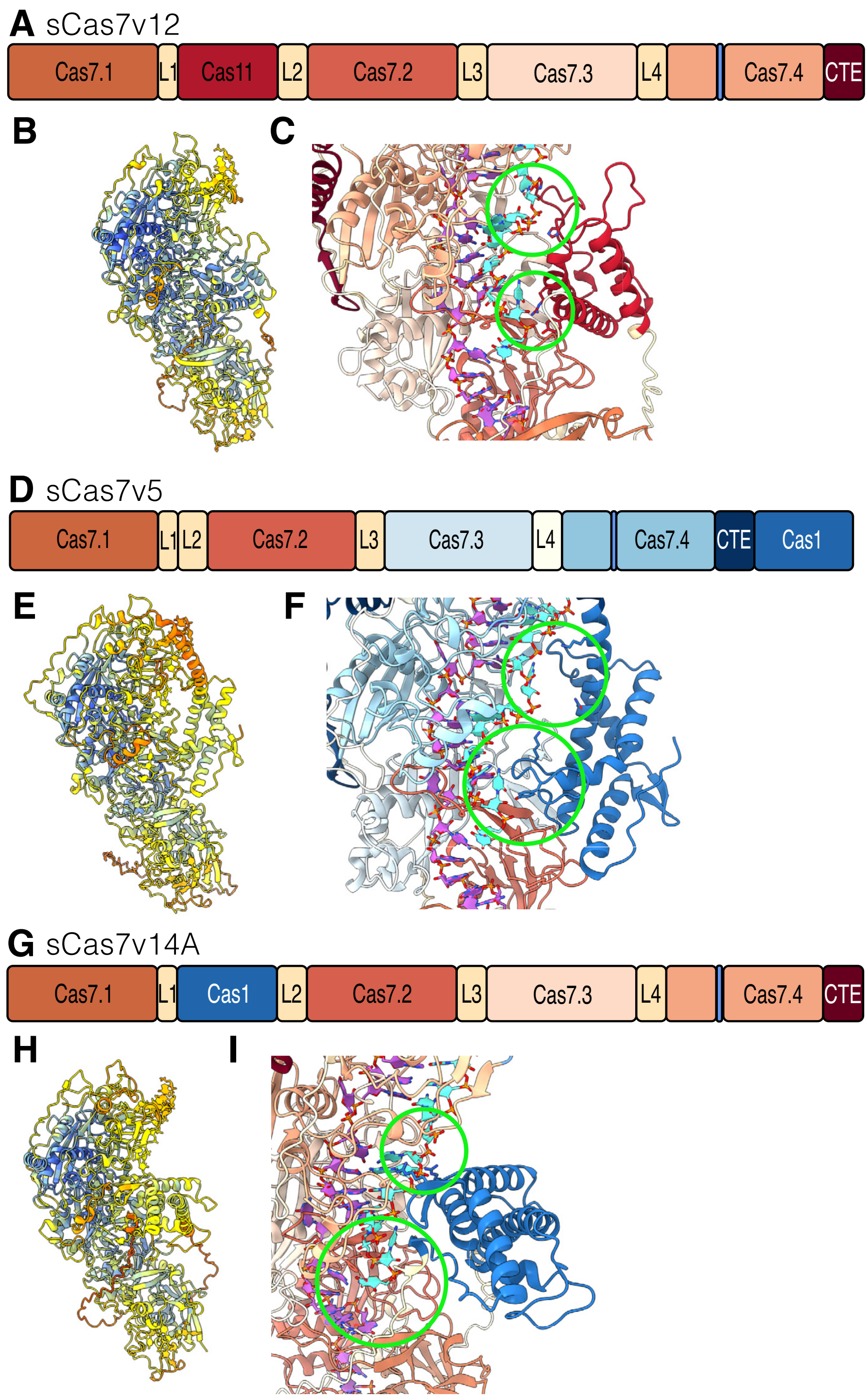
A sCas7v12
Cas7.1
L1
Cas11
L2
Cas7.2
L3
Cas7.3
L4
Cas7.4
CTE
B
C
D sCas7v5
Cas7.1
L1
L2
Cas7.2
L3
Cas7.3
L4
Cas7.4
CTE
Cas1
E
F
G sCas7v14A
Cas7.1
L1
Cas1
L2
Cas7.2
L3
Cas7.3
L4
Cas7.4
CTE
H
I

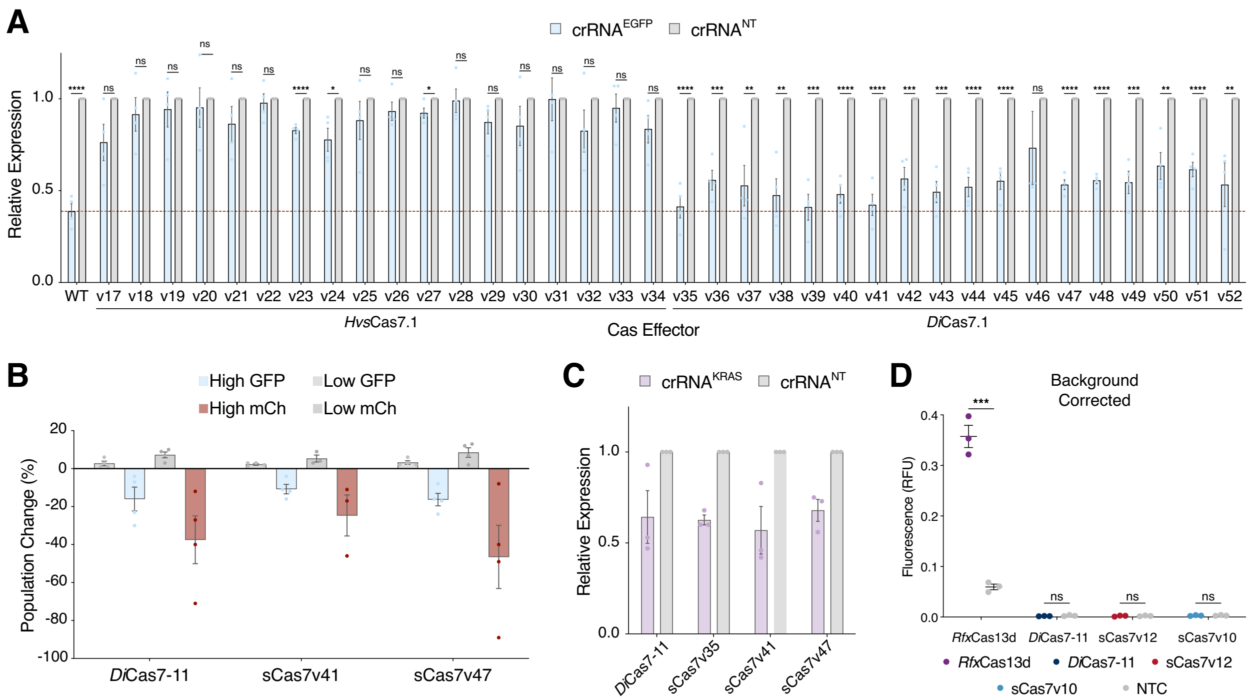

Figure 6. Generation and validation of compact sCas7 effectors. (**A**) Schematic depicting workflow for analysis of sCas7 library with refined ODS design method. (**B**) qPCR analysis of EGFP knockdown with all 36 compact sCas7 effectors. Data is broken into two groups *Hvs*Cas7.1-based (v17-v34) and *Di*Cas7.1-based (v35-v52) sCas7 effectors. Dashed red line represents average knockdown by *Di*Cas7-11 (WT). Significance is calculated and determined using unpaired *t*-test between crRNA^{EGFP} and crRNA^{NT}. WT = wild-type *Di*Cas7-11. Error bars represent sem (n = 4). (**C**) Flow cytometry analysis of select Cas7-S effectors demonstrating effect of RNA knockdown on translation of EGFP and mCherry. Data depicts population change in High or Low GFP, or mCherry, expression groups (see methods for gating). Error bars represent sem (n = 4). (**D**) RNA knockdown of KRAS gene with DiCas7-11 and select Cas7-S effectors analyzed using qPCR. Error bars represent SEM (n = 3). (**E**) SENSR assay determining ssRNA collateral activity of sCas7 effectors depicted by background corrected fluorescence levels. *Rfx*Cas13d was used as a positive control. Error bars represent sem (n = 3). RFU = relative fluorescence unit.

domain), and sCas7v41 (with the HvsCas11 domain) demonstrated knockdown comparable to WT *Di*Cas7-11 (Figure S5D). The variant sCas7v41 was the most compact (1241AA) due to the smaller size of the *Hvs*Cas domains and represents the smallest type III-E effector developed (Figure S5C).

The sCas7 variants were also assayed for their ability to reduce the expression of target proteins using a flow cytometry assay for knockdown of

Figure 5. Structural comparison between three smaller active sCas7 molecules modeled by AlphaFold3. (**A**) Schematic of the domain structure of sCas7v12 which is wild type *Di*Cas7-11 without the INS domain. (**B**) Structure of the ternary structure of sCas7v12 with crRNA and tgRNA colored according to the AlphaFold3 pIDDT score. (**C**) Zoom-in of the Cas7.2 and Cas7.3 active sites showing the Cas11 domain. Circles show the scissile phosphates with nearby basic residues from the Cas11 domain shown in sticks (H306, H312 near Cas7.3 catalytic site and R283, Y360 near Cas7.2 catalytic site). (**D**) Schematic of the domain structure of sCas7v5 which consists of Cas7.1 and 7.2 domains from *Di*Cas7-11 fused to Cas7.3 and 7.4 and Cas1 domains from Cas7-1. (**E**) Structure of the ternary structure of sCas7v5 with crRNA and tgRNA colored according to the AlphaFold3 pIDDT score. (**F**) Zoom-in of the Cas7.2 and Cas7.3 active sites showing the Cas1 domain. Circles show the scissile phosphates with nearby basic residues from the Cas1 domain shown in sticks (K1193 near Cas7.3 catalytic site and Y1233, K1237 near Cas7.2 catalytic site). (**G**) Schematic of the domain structure of sCas7v14a which consists of Cas7.1, 7.2, 7.3, and 7.4 domains from *Di*Cas7-11 but has the Cas7-1 Cas1 domain in place of the *Di*Cas7-11 Cas11 domain. (**H**) Structure of the ternary structure of sCas7v14a with crRNA and tgRNA colored according to the AlphaFold3 pIDDT score. (**I**) Zoom-in of the Cas7.2 and Cas7.3 active sites showing the Cas1 domain. Circles show the scissile phosphates with nearby basic residues from the Cas1 domain shown in sticks (R333 near Cas7.3 catalytic site and R412 near Cas7.2 catalytic site).

EGFP and mCherry (Figure S6). This assay tests whether, like the wild-type Cas7-11, variants can knock-down multiple target RNAs simultaneously. Variants sCas7v41 and sCas7v47 were comparable to *Di*Cas7-11 for both targets tested (Figure 6B). Furthermore, the sCas7 variants are capable of knocking down endogenous genes as effectively as *Di*Cas7-11 (Figure 6D). As expected, based on previous reports [3], the sCas7-variants did not have the collateral cleavage activity that was found in Cas13 CRISPR-based RNA-targeting systems (Figure 6D).

Discussion

Cas7-11 proteins are the largest single-effector Cas protein family discovered [2,3]. They are advantageous because they do not have collateral cleavage activity, however, they are beyond or near the size limit for translatable delivery systems [5]. Here we explored the possibility that the Cas7 domains from one ortholog could be substituted for those from another ortholog. In addition, the roles and placement of the Cas1 and Cas11 domains within the overall protein architecture were studied. We used orthogonal domain substitution (ODS) to generate synthetic type III-E effectors capable of RNA-targeting. The ODS method reveals a unique modularity of the type III-E effector class. By mixing and matching the domains from two different Cas7-11 proteins with those from the inactive Cas7-1, several important features of these modular proteins were discovered.

A very small Cas7-based protein, discovered by bioinformatics search, was found to be inactive, likely due to its lack of a Cas7.1 domain and the N-terminal part of the Cas7.2 domain. Adding back the Cas7.1 and Cas7.2 domains from *Di*Cas7-11 rescued its activity, indicating that fusing Cas7 domains with those from another species is a viable engineering approach.

Once RNA-knockdown activity was regained, the function of the other domains could be analyzed. The main structural difference between Cas7-1 and Cas7-11 was that the Cas1 domain in Cas7-1 is at the C-terminus of Cas7-1 whereas the Cas11 domain in *Di*Cas7-11 is between the Cas7.1 and Cas7.2 domains. The Cas1 domain of Cas7-1 and has no sequence similarity or predicted structural similarity to the Cas11 domain from *Di*Cas7-11. Despite a lack of similarity, Cas1 permitted RNA-knockdown when constructs (e.g. sCas7v1-3, sCas7v5-9) lacked the Cas11 domain even when positioned at the C-terminus as observed in the original Cas7-1 architecture. Moreover, the Cas1 domain could be inserted between the Cas7.1 and Cas7.2 domains in place of the Cas11 domain (sCas v13-14, v16) to generate active proteins. However, when the Cas7.3 and Cas7.4 domains were from Cas7-1 (sCas7v15), this substitution did not result in an active protein. Activity was improved by removing either the first 21 amino acids or 29 amino acids from the N-terminus of the Cas1 domain across all variants (sCasv13-16) using Cas1 in place of Cas11 with sCas7v14A being as effective at RNA-knockdown as the WT *Di*Cas7-11. Although no structures are currently available for these chimeric proteins, AlphaFold models showed that the Cas1 and the Cas11 domain embedded between the Cas7.1 and Cas7.2 domains adopt similar positions near scissile phosphates to facilitate tgRNA cleavage. Activity was obtained even when the Cas1 is positioned at the C-terminus as it is in Cas7-1. In all models, the Cas1 domain is located in the same position as the Cas11 domain in *Di*Cas7-11 (Figure 5).

Another main conclusion from our study is that the catalytic domains, Cas7.2 and Cas7.3, are interchangeable and domains from any species appear to permit tgRNA cleavage. This observation aligns well with previous work showing that the *Di*Cas7.1 domain is sufficient for crRNA binding [4]. Our result shows that the sCas7 variants will likely be extremely useful for cleavage of a wide variety of target sequences.

Finally, we note that by starting with Cas7-1, adding the domains required for activity, and then mixing in smaller Cas7 domains from other species, we reduced the size of the starting DiCas7-11 of 1601 amino acids to 1241 amino acids in the smallest active sCas7 variant, sCas7v41. This protein is within the limit that could be encoded in adenovirus for gene therapy applications [29]. In conclusion, Cas7-11 proteins are modular and can be engineered into compact, efficient, and highly specific sCas7 effectors for RNA-targeting applications.

Methods

Bioinformatics

Cas7-1 was identified through BLAST queries of type III-E CRISPR-Cas effectors (MBU1487208.1). The amino acid sequence of Cas7-1 was submitted to HHPred for individual domain assignment (https://toolkit.tuebingen.mpg.de/tools/hhpred). Assumed DRs of Cas7-1 were identified by submitting metagenomic data related to Cas7-1 to CRISPR-Cas++ (https://crisprcas.i2bc.paris-saclay.fr/). DR secondary structure prediction was obtained using UNAFold (https://www.unafold.org/). To determine domain boundaries for the different type III-E CRISPR-Cas effectors a multiple sequence alignment was performed on all of the sequences from Table S1 using Clustal Omega. Table S1 shows the number of amino acids in each domain compared to *Di*Cas7-11. All amino acids in each protein were accounted for in the domain assignments. HHPred was performed on the full Cas7-1 sequence and individual domains of Cas7-1 to identify homologous proteins with known structures that mapped to individual Cas7-1 domains. The search identified high probability hits. Data is sorted by domain and up to highest scoring 15 results were presented in Table S1.

Design and cloning of constructs

Plasmids for expression of effectors in HEK293T cells were designed with a CMV promoter and bovine growth hormone (bGH) terminator. Effector plasmids were generated using standard Gibson assembly methods. crRNA plasmids were designed for expression driven by a U6 promoter and terminator. crRNA expression plasmids were generated using standard golden gate assembly methods. Select plasmids are available at https://www.addgene.org/ (Table S4).

Recombinant protein expression and purification

Plasmids used for protein expression in *E. coli* were generated by subcloning ORFs from plasmids used for mammalian cell culture expression, along with an N-terminal 6xHis-SUMO into a pET28a vector backbone. Plasmids were then transformed into Rosetta™ 2(DE3)pLysS Competent Cells (Novagen). Single colonies were used to inoculate a 40 mL LB overnight starter culture. The starter cultures were then transferred to a 1L LB culture in 4L baffled flasks and grown at 37 °C with shaking (200 rpm) until A_{600} reached ~1.0. Cultures were then brought to 4 °C before protein expression was induced with 0.2 mM isopropyl β-D-thiogalactopyranoside (IPTG) and grown for 18–20 h at 18 °C. Cells were then pelleted and resuspended in a lysis buffer containing 50 mM Tris–HCl pH 8.0, 300 mM NaCl, 10 mM imidazole, 5% glycerol (v/v), and 3 mM β-mercaptoethanol supplemented with Protease Inhibitor Cocktail (Sigma P2714), 5 mM PMSF, and 2.5 U/mL salt active nuclease (Sigma SRE0015). Cells were lysed via sonication and clarified by centrifugation. His-tagged protein was bound to 2 mL HisPur™ Ni-NTA Resin (Thermo 88221) equilibrated with lysis buffer in a glass Econo-Column® Chromatography Columns (Bio-Rad) by flowing through the clarified lysate. A wash step was then performed by adding 12 column volume (CV) of a wash buffer containing 50 mM Tris–HCl pH 8.0, 500 mM NaCl, 30 mM imidazole, and 5% glycerol followed by elution with 7 CV elution buffer containing 50 mM Tris–HCl pH 8.0, 300 mM NaCl, 300 mM imidazole, and 5% glycerol. The 6xHis-SUMO tag was cleaved off by dialyzing the eluate overnight at 4 °C with ~0.6 mg of in-house produced 6xHis-tagged Ulp1 (Yeast SUMO Protease) in a dialysis buffer containing 20 mM HEPES-NaOH pH 7.5, 250 mM NaCl, 5% glycerol, and 1 mM DTT. Dialyzed sample was then flowed over the same Ni-NTA column equilibrated in a buffer containing 20 mM HEPES-NaOH pH 7.5, 250 mM NaCl, 25 mM imidazole, 5% glycerol, and 1 mM DTT to remove additional *E. coli* impurities, Ulp1, and the 6xHis-SUMO tag. Cation exchange chromatography was performed with 2 × 1 mL HiTrap Heparin HP Column (Cytiva) with a NaCl gradient from 200 to 1000 mM NaCl followed by gel filtration chromatography with a HiLoad 16/600 Superdex 200 column equilibrated in 20 mM HEPES-NaOH pH 7.5, 600 mM NaCl, 5% glycerol (v/v), 2 mM DTT on an ÄKTA Pure (Cytiva). Proteins were then concentrated to ~10 μM and stored in small aliquots at −80 °C for future use.

Nucleic acid target and crRNA preparation

Synthetic ssRNA templates and the full DiCas7-11 crRNA array were ordered custom from IDT. All other crRNAs were produced in house. To generate crRNAs, a dsDNA template with a T7 promoter incorporated was produced through template-less PCR and purified with MinElute PCR Purification Kit (Qiagen 28004). dsDNA templates were converted to ssRNA through *in vitro* transcription using MEGAScript™ T7 Transcription Kit (Invitrogen AM1334) and purified with MEGAClear™ Transcription Clean-Up Kit (Invitrogen AM1908).

Mammalian cell culture

HEK293T cell lines were obtained from the American Type Culture Collection (ATCC CRL-3216) and used in all mammalian cell experiments. HEK293T cells were cultured in Dulbecco's Modified Eagle Medium (DMEM) (Thermo Fisher Scientific 11995073) supplemented with 10% Fetal Bovine Serum (FBS) (Corning 35-011-CV) and 1% penicillin–streptomycin (Thermo Fisher Scientific 15070063). Transient transfections were carried out with Lipofectamine 3000 (Thermo Fisher Scientific L3000001) according to the manufacturer's protocol.

RNA-knockdown assay

To assess RNA knockdown, we used an assay in which three plasmids were transfected. One contained a crRNA that would down-regulate EGFP or mCherry. The second plasmid coded for one of the variant Cas effectors. The third plasmid was the EGFP or mCherry reporter plasmid. If the variant Cas effector is able to cleave the RNA transcript from the reporter plasmid, then the fluorescence signal is less than for a control wherein the crRNA is a control non-targeting sequence. HEK293T cells were co-transfected with 20 ng of either the EGFP or mCherry reporter plasmid, 600 ng of a respective Cas effector plasmid, and 300 ng of crRNA plasmid. The sequences of the various crRNAs are given in Table S3. Cells were seeded in 48-wells 18–20 h prior to transfection at seeding densities of 32,000 cells per well. Following transfection, cells were incubated for 48 h at 37 °C, 5% CO_2. After 48 h, cells were removed from the plate with 250 μL of RNAprotect Cell Reagent (Qiagen 76104) and stored at −20 °C for at least 24 h prior to extraction. RNA knockdown of the fluorescent proteins was assessed by flow cytometry (see below). RNA amounts were quantitated after cell lysis and subsequent qPCR as described below. For each effector tested, four biological replicates were performed, and a non-target crRNA was used as a control.

Total RNA collection and qPCR

To measure the reduction of endogenous or reporter genes, the transfected cells, preserved in RNAprotect, were lysed using QIAshredder (Qiagen 79656). Total RNA was then extracted using the RNeasy Mini Kit (Qiagen 74106) according to the manufacturer's protocol. Following extraction, the total RNA was treated with DNase (Thermo Fisher Scientific AM1907) to remove any remaining DNA. Sample RNA concentration was analyzed using a Nanodrop OneC UV–vis spectrophotometer (Thermo Fisher Scientific NDONEC-W). Approximately 0.5 μg of total RNA was used to synthesize cDNA with a RevertAid First Strand cDNA Synthesis Kit (Thermo Fisher Scientific K1622). cDNA was diluted (1:1000) for qPCR analysis. qPCR was performed with SYBR green (qPCRBIO SyGreen Blue Mix Separate-ROX 17-507B, Genesee Scientific), using 4 μl of dilute cDNA in each 20 μl reaction containing a final primer concentration of 200 nM and 10 μl of SYBR green buffer solution. Three technical replicates were performed for each reaction. Pipetting was performed using EpMotion® 5075 (Eppendorf). The following qPCR protocol was used on the LightCycler® 96 (Roche): 3 min of activation phase at 95 °C, 40 cycles of 5 sec at 95 °C, and 30 sec at 60 °C. The relative expression levels of EGFP were calculated using the manufacturer's software and the delta-delta Ct method (2–ΔΔCt), with the GAPDH gene serving as a Ref. [30]. To assess differences in EGFP expression between the non-target and targeting crRNA conditions for each effector, statistical analysis was performed using GraphPad Prism 10. Specifically, data were analyzed using an unpaired *t*-test.

Flow cytometry

Fluorescence knockdown was assessed using flow cytometry on the BioRad S3e cell sorter system. To prepare cells for analysis, transfected HEK293T cells were washed with PBS pH 7.4 (Gibco 10010031), all media was removed, then 40 μL of Accumax (VWR AM105) was added to the well. 230 μL of cold PBS pH 7.4 was added to the wells and cells were resuspended and transferred to a cell strainer (Corning 352235). Cells were then assessed on the S3e cell sorter with a count of 80,000 cells per sample. Flow cytometry data were analyzed using Floreada.io (https://floreada.io/) (Figure S9).

Nuclease assays

Nuclease assays were run in 10 μL reactions with the following final concentrations: 500 nM protein, 200 nM crRNA, 240 nM probe, 40U RNase Inhibitor, and 10 mM $MgCl_2$. Reactions were supplemented with a custom 10X reaction buffer (200 mM HEPES (pH 7.5), 600 mM NaCl) and incubated at 37 °C. Times were varied in different experiments. Upon completion, reactions were denatured with 2X RNA dye (NEB B0363S) at 95 °C for 10 min. 10 μl of dyed samples were loaded onto a pre-run (200 V for 60 min) 15% TBE-Urea PAGE gel (BioRad 4566055) and resolved at 200 V for 35 min. Gels were then stained with SYBR Gold (Invitrogen S11494) and incubated for 10 min at room temperature on a shaker and washed in 1X TBE for 10 min on a shaker. Stained gels were imaged using Enduro™ GDS (Labnet).

To assay for collateral cleavage, SENSR reactions were performed to compare sCas7 variants to RfxCas13d as previously described [31]. If collateral cleavage occurs, a bystander ssRNA probe is cleaved. The ssRNA probe is conjugated to 6-FAM, and a fluorescence quencher so that an increase in 6-FAM fluorescence is observed if the RNA is cleaved resulting in increased distance between the quencher and the 6-FAM. In the assay performed here, 100 nM of RfxCas13d or 200 nM of *Di*Cas7-11 or sCas7variant was used in the reaction.

Structure prediction

Structural models of all of the constructs were prepared using AlphaFold2 in order to guide interpretation of experimental results. Finally, AlphaFold3 was used to visualize three of the models with both crRNA and tgRNA bound. These models were sCas7v12, which consists of all *Di*Cas domains but did not contain the INS, sCas7v5, which has the Cas1 domain at the C-terminus of the protein) and sCas7v14a (which has the Cas1 domain in place of the *Di*Cas Cas11 domain inserted between the Cas7.2 and Cas7.3 domains.

CRediT authorship contribution statement

Daniel J. Brogan: Writing – review & editing, Writing – original draft, Methodology, Investigation, Formal analysis, Conceptualization.

Calvin P. Lin: Investigation. **Elena Dalla Benetta:** Investigation. **Tianqi Wang:** Investigation. **Fangying Chen:** Investigation. **Harry Li:** Investigation. **Claire Lin:** Investigation. **Elizabeth A. Komives:** Writing – review & editing, Writing – original draft, Formal analysis. **Omar S. Akbari:** Writing – review & editing, Writing – original draft, Supervision.

DATA AVAILABILITY

Select plasmids have been sent to Addgene and will be available for ordering. For other plasmids not found on Addgene, please submit a request to OSA.

DECLARATION OF COMPETING INTEREST

The authors declare the following financial interests/personal relationships which may be considered as potential competing interests: Omar S. Akbari reports a relationship with Synvect Inc. that includes: equity or stocks. Omar S. Akbari reports a relationship with Agragene Inc. that includes: equity or stocks. Daniel J. Brogan has patent pending to University of California San Diego. If there are other authors, they declare that they have no known competing financial interests or personal relationships that could have appeared to influence the work reported in this paper.

Acknowledgments

This work was supported by NIH/NIAID (R01GM-132825-04, R21RAI149161A, RO1AI1900001 and DP2AI152071) awarded to OSA. Thank you to the members of the Komor lab for advice in establishing systems for assay development and providing template plasmids essential to experimentation. We would also like to thank Kevin Corbett for his critical advice provided.

Appendix A. Supplementary material

Supplementary material to this article can be found online at https://doi.org/10.1016/j.jmb.2025.169566.

Received 7 July 2025;
Accepted 24 November 2025;
Available online 27 November 2025

Keywords:
type III-E effectors;
CRISPR-Cas;
protein engineering;
RNA knockdown

† Equal first author contributions.

References

[1]. Makarova, K., Wolf, Y., Iranzo, J., Shmakov, S., Alkhnbashi, O., Brouns, S., et al., (2020). Evolutionary classification of CRISPR-Cas systems: a burst of class 2 and derived variants. *Nature Rev. Microbiol.* **18**, 67–83.
[2]. van Beljouw, S., Haagsma, A., Rodríguez-Molina, A., van den Berg, D., Vink, J., Brouns, S., (2021). The gRAMP CRISPR-Cas effector is an RNA endonuclease complexed with a caspase-like peptidase. *Science* **373**, 1349–1353.
[3]. Özcan, A., Krajeski, R., Ioannidi, E., Lee, B., Gardner, A., Makarova, K.S., et al., (2021). Programmable RNA targeting with the single-protein CRISPR effector Cas7-11. *Nature* **597**, 720–725.
[4]. Goswami, H.N., Rai, J., Das, A., Li, H., (2022). Molecular mechanism of active Cas7-11 in processing CRISPR RNA and interfering target RNA. *Elife* **11**, e81678.
[5]. Kato, K., Zhou, W., Okazaki, S., Isayama, Y., Nishizawa, T., Gootenberg, J.S., et al., (2022). Structure and engineering of the type III-E CRISPR-Cas7-11 effector complex. *Cell* **185**, 2324–2337.e16.
[6]. Hu, C., van Beljouw, S.P.B., Nam, K.H., Schuler, G., Ding, F., Cui, Y., et al., (2022). Craspase is a CRISPR RNA-guided, RNA-activated protease. *Science* **377**, 1278–1285.
[7]. Buchman, A.B., Brogan, D.J., Sun, R., Yang, T., Hsu, P. D., Akbari, O.S., (2020). Programmable RNA targeting using CasRx in flies. *CRISPR J.* **3**, 164–176.
[8]. Bot, J., van der Oost, J., Geijsen, N., (2022). The double life of CRISPR-Cas13. *Curr. Opin. Biotechnol.* **78**, 102789.
[9]. Kelley, C., Haerle, M., Wang, E., (2022). Negative autoregulation mitigates collateral RNase activity of repeat-targeting CRISPR-Cas13d in mammalian cells. *Cell Rep.* **40**, 111226.
[10]. Wang, Q., Liu, X., Zhou, J., Yang, C., Wang, G., Tan, Y., et al., (2019). The CRISPR-Cas13a gene-editing system induces collateral cleavage of RNA in glioma cells. *Adv. Sci.* **6**, 1901299.
[11]. Kato, K., Okazaki, S., Schmitt-Ulms, C., Jiang, K., Zhou, W., Ishikawa, J., et al., (2022). RNA-triggered protein cleavage and cell growth arrest by the type III-E CRISPR nuclease-protease. *Science* **378**, 882–889.
[12]. Ekundayo, B., Torre, D., Beckert, B., Nazarov, S., Myasnikov, A., Stahlberg, H., et al., (2023). Structural insights into the regulation of Cas7-11 by TPR-CHAT. *Nature Struct. Mol. Biol.* **30**, 135–139.
[13]. Huo, Y., Zhao, H., Dong, Q., Jiang, T., (2023). Cryo-EM structure and protease activity of the type III-E CRISPR-Cas effector. *Nature Microbiol.* **8**, 522–532.
[14]. Hale, C., Zhao, P., Olson, S., Duff, M., Graveley, B., Wells, L., et al., (2009). RNA-guided RNA cleavage by a CRISPR RNA-Cas protein complex. *Cell* **139**, 945–956.
[15]. Babu, M., Beloglazova, N., Flick, R., Graham, C., Skarina, T., Nocek, B., et al., (2011). A dual function of the CRISPR-Cas system in bacterial antivirus immunity and DNA repair. *Mol. Microbiol.* **79**, 484–502.
[16]. Silas, S., Mohr, G., Sidote, D., Markham, L., Sanchez-Amat, A., Bhaya, D., et al., (2016). Direct CRISPR spacer acquisition from RNA by a natural reverse transcriptase–Cas1 fusion protein. *Science* **351**, aad4234.
[17]. Nuñez, J., Kranzusch, P., Noeske, J., Wright, A., Davies, C., Doudna, J., (2014). Cas1-Cas2 complex formation

mediates spacer acquisition during CRISPR-Cas adaptive immunity. *Nature Struct. Mol. Biol.* **21**, 528–534.

[18]. Forslund, K., Pekkari, I., Sonnhammer, E., (2011). Domain architecture conservation in orthologs. *BMC Bioinf.* **12**, 326.

[19]. Varadi, M., Anyango, S., Deshpande, M., Nair, S., Natassia, C., Yordanova, G., et al., (2022). AlphaFold protein structure database: massively expanding the structural coverage of protein-sequence space with high-accuracy models. *Nucleic Acids Res.* **50**, D439–D444.

[20]. Jumper, J., Evans, R., Pritzel, A., Green, T., Figurnov, M., Ronneberger, O., et al., (2021). Highly accurate protein structure prediction with AlphaFold. *Nature* **596**, 583–589.

[21]. Cianfrocco, M., Wong-Barnum, M., Youn, C., Wagner, R., Leschziner, A., (2017). COSMIC2: a science gateway for cryo-electron microscopy structure determination. In: Machinery, A.F.C. (Ed.), *Proceedings of the Practice and Experience in Advanced Research Computing 2017 on Sustainability, Success and Impact*.

[22]. Wang, S., Guo, M., Zhu, Y., Lin, Z., Huang, Z., (2022). Cryo-EM structure of the type III-E CRISPR-Cas effector gRAMP in complex with TPR-CHAT. *Cell Res.* **32**, 1128–1131.

[23]. Yu, G., Wang, X., Zhang, Y., An, Q., Wen, Y., Li, X., et al., (2022). Structure and function of a bacterial type III-E CRISPR-Cas7-11 complex. *Nature Microbiol.* **7**, 2078–2088.

[24]. Liu, X., Zhang, L., Wang, H., Xiu, Y., Huang, L., Gao, Z., et al., (2022). Target RNA activates the protease activity of Craspase to confer antiviral defense. *Mol. Cell* **82**, 4503–4518.

[25]. Lin, C., Li, H., Brogan, D., Wang, T., Akbari, O., Komives, E., (2025). CRISPR RNA binding drives structural ordering that primes Cas7-11 for target cleavage. *Nucleic Acids Res.* **53**, gkaf271.

[26]. Strecker, J., Demircioglu, F.E., Li, D., Faure, G., Wilkinson, M.E., Gootenberg, J.S., et al., (2022). RNA-activated protein cleavage with a CRISPR-associated endopeptidase. *Science* **378**, 874–881.

[27]. Zheng, Y., Li, J., Wang, B., Han, J., Hao, Y., Wang, S., et al., (2020). Endogenous type I CRISPR-Cas: from foreign DNA defense to prokaryotic engineering. *Front. Bioeng. Biotechnol.* **8**, 62.

[28]. Liu, T.Y., Doudna, J.A., (2020). Chemistry of Class 1 CRISPR-Cas effectors: Binding, editing, and regulation. *J. Biol. Chem.* **295**, 14473–14487.

[29]. Bennett, A., Mietzsch, M., Agbandje-McKenna, M., (2017). Understanding capsid assembly and genome packaging for adeno-associated viruses. *Future Virol.* **12**, 283–297.

[30]. Adeola, F., (2018). Normalization of gene expression by quantitative RT-PCR in human cell line: comparison of 12 endogenous reference genes. *Ethiop. J. Health Sci.* **28**, 741–748.

[31]. Brogan, D., Chaverra-Rodriguez, D., Lin, C., Smidler, A., Yang, T., Alcantara, L., et al., (2021). Development of a rapid and sensitive CasRx-based diagnostic assay for SARS-CoV-2. *ACS* **6** (11), 3957–3966.